

Explosive Welding of Light Weight Metal Sheets

Yamato MATSUI¹, Masahiko OTSUKA¹, Takeshi HINATA¹
Erik CARTON², Shigeru ITOH³

¹Graduate School of Science and Technology, Kumamoto University 2-39-1 Kurokami,
Kumamoto City, Kumamoto 860-8555, Japan

²TNO-Prins Maurits Laboratory, P.O. Box 45, 2280AA Rijswijk, The Netherlands

³Shock Wave and Condensed Matter Research Center, Kumamoto University, 2-39-1 Kurokami,
Kumamoto City, Kumamoto 860-8555, Japan

1. Abstract

The technique of explosive line welding is one of the processing techniques and it can connect similar and dissimilar metal sheets using large energy of explosive during very short time. In this study we try to weld lightweight metal sheets by experiment and work on the numerical simulation concerning a series of the phenomenon. Materials involved are aluminum alloys Al5052-O, 6061T6 and 6M83, magnesium alloy AZ31B-O and commercially pure titanium TP270C.

After welding samples were taken to perform shear strength test and the welding interface was analyzed using optical microscopy. The strength test indicates a remarkable good bonding between similar welded metals. Particularly, the use of line welding shows a high strength to explosive mass ratio, making it a good candidate to be scaled up and used in commercial applications.

2. Introduction

The car body is hoped to use lightweight metals like aluminum, magnesium and titanium alloy in recent years. Now some company produce the cars made from aluminum alloys. But these cars are used rivets for connecting method between both metal sheets. If it succeeds the explosive welding between both similar and dissimilar lightweight metal sheets, the car can be made without rivets and it is enable to develop superior products.

In this study we try to the welding between similar and dissimilar light weight metal plates by experiment and numerical simulation. Materials involved are aluminum alloys Al5052-O, 6061T6, 6M83-T4 and 7075-T6, magnesium alloy AZ31B-O and commercially pure titanium TP270C.

Solid state welding at room temperature is necessary in order to avoid the forming of intermetallics. All metals used in this research are very reactive towards each other. Furthermore, the Aluminum and the Magnesium alloys have a low melting point. In order to reduce the mass transport of atoms (avoid high temperature and specially melting), the wave formation during the welding process should be closely controlled or maybe even avoided. This will reduce the temperature of the welding interface and hopefully avoid the forming of brittle intermetallics at the welding interface.

3. The Fundamental Configuration and Principle of Explosive Welding

The fundamental configuration and principle of explosive welding are shown in figure 1. It is drawn the case of the connection between both metal plates here. The key of explosive welding is to impact flyer plate to base plate with one proper impact angle. Then the metal jet is generated at the collision point, and it clean the surface of flyer and base plate with eliminates function. And next time, the high pressure by impact is approached the both metal to bonding area of atom and atom. This process accomplishes the explosive welding.

The detonation velocity V_d , the flyer velocity V_p and the impact angle β have a geometric relation each other. The flyer velocity and impact angle are important cause to accomplish the preferable welding. The weldability window of explosive welding (the relation of V_p and β) is shown in figure 2. It products the wavy bonding line between both plates in this range. And in some case of V_p and β it produced smooth boundary face. The bonding area is not melted, also there is not the diffusion for component element of flyer and base material at the bonding area. The weldability window explosive welding (the relation of V_c and β) is shown in figure 3. If we work on the experiment at the condition within these weldability windows, we can obtain the desirable bonding sample.

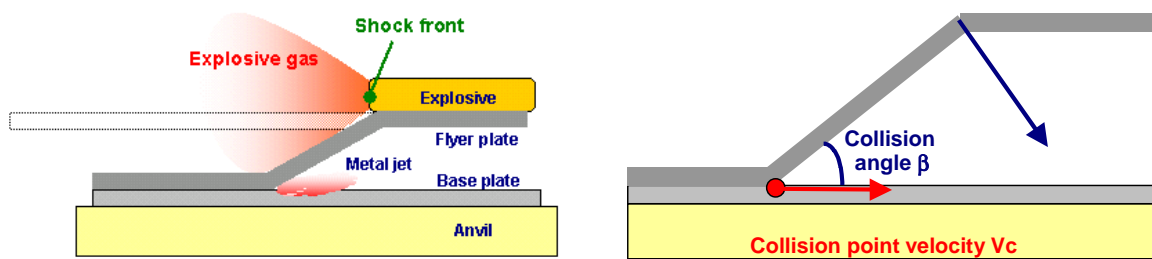
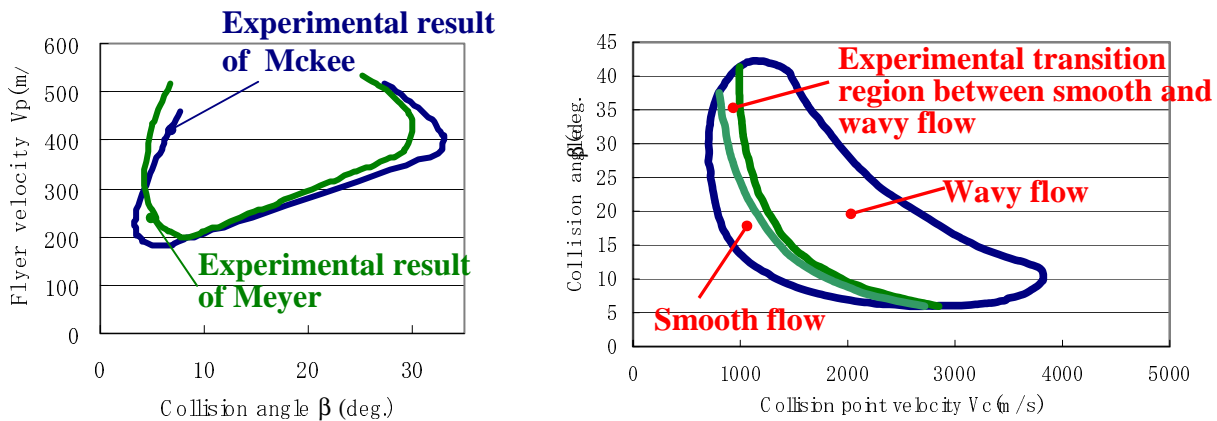


Figure 1. The fundamental configuration and principle of explosive welding



(Left) Figure 2. Weldability window of explosive welding (the relation of β and V_p)
 (Right) Figure 3. Weldability window of explosive welding (the relation of β and V_c)

4. Experiment of Explosive Line Welding

We suggest the explosive line welding method that is one technique of explosive welding using the detonation cord with 10g/m PETN. The character of this method is to connect the two metal plates with line form. The experimental set up is shown in figure 4. The detonation cord of cylindrical form was placed parallel on the edge area of flyer plate and little stand off was set between the flyer and base metal plate. The flyer and base plates were crossed about 10mm from the edge of plate each other and electric detonator detonated the cord.

First welding experiments with similar metal combinations were performed as they are expected to be easier weld since there is no chance for the formation of brittle intermetallic phases. As a second step, we have performed tests on the welding of dissimilar metal combinations. Before welding, all plates were slightly grained and cleaned with ethanol over the part of their surfaces to be weld.

Figure 5 shows the schematic representation of line weld. Upon detonation it causes a localized line weld between the two metals on both sides, just next to the detonation cord, where an inclined collision occurs. As soon as the velocity of the collision line becomes subsonic, jetting occurs, resulting in the typical wave pattern as shown in this figure. The cross section reveals the typical wave pattern that exists on each side of the detonation cord.

One side of the line welding obtained by an experiment is shown in figure 6. The upper side material is Ti TP270C and the under side material is Al 6061-T6 in this figure. We can observe the wavy interface from this photograph and this result indicates the strong connection with two plates.

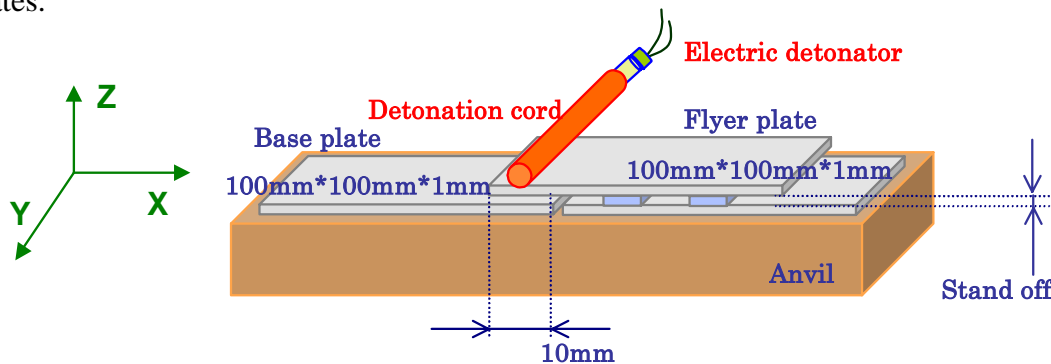


Figure 4. The experimental set up of explosive line welding

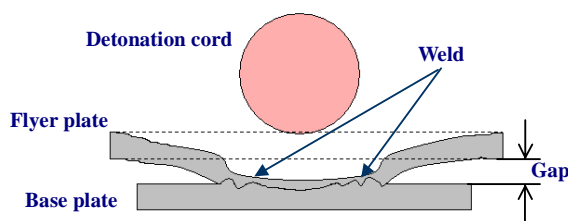


Figure 5. Schematic representation of line welding



Figure 6. One side of the line welding of Ti TP270C to Al 6061-T6

The experimental condition and the results of strength test about similar metal combinations are shown in table 1. Also the experimental condition of dissimilar metal combinations and the results are shown in table 2.

Table 1. The experimental condition and the results of strength test about similar metal combinations

Metal combination		Stand off	Bonding	Shear strength (MPa)	Weld break
Al 5052-O	AA5052-O	0.5mm	Yes	41	No
Al 6061-T6	AA6061-T6	0.6mm	Yes	42	No
6M83-T4	6M83-T4	0.6mm	Yes	44	No
Ti TP270C	Ti TP270C	0.3mm / 0.6mm	No / Yes	66	No
MgAZ31B-O	MgAZ31B-O	0.8mm	Yes	15	Yes

Table 2. The experimental condition of dissimilar metal combinations and the results

Metal combination (flyer / base)		Stand off	Bonding
Al 5052-O	Ti TP270C	0.7	Yes
Al 5052-O	MgAZ31B-O	0.5	No
Al 6061-T6	Ti TP270C	0.6	Yes
Al 6061-T6	MgAZ31B-O	0.6	No
6M83-T4	Ti TP270C	0.6	Yes
6M83-T4	MgAZ31B-O	0.5	No

It is known that the strength of bonding area by explosive welding becomes stronger than the one of only base plate. It indicates that the bonding area is stronger than the other area if the break area is not bonding area. Conversely the welding is not enough if bonding area break at first. The results of strength tests show that in case of similar metal combinations the bonded zone was stronger than the bulk material in tension except MgAZ31B-O. Probably due to a large bonded area compared to the cross section of the sheets. Frequently, necking occurred away from the lap joint and not the strength value of the weld was obtained, but the stress-strain curve of the starting material. Only a minimum shear strength value for the weld zone could be calculated from these results.

5. Numerical Simulation of Explosive Line Welding

The numerical simulation model is shown in Figure 7 We calculated this series of phenomenon for explosive line welding by using an explicit finite element code, LS-DYNA3D. The details of calculation method are shown in the following.

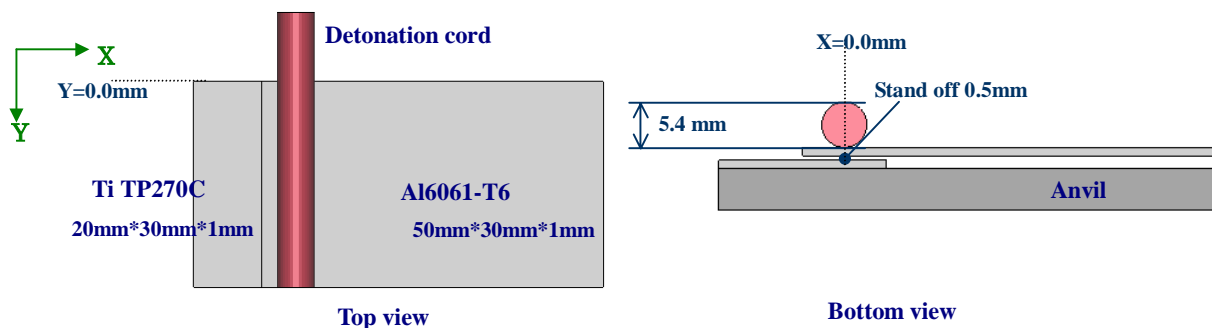


Figure 7. The numerical simulation model of explosive line welding

EOS JWL

The equation of state for an explosive in this study was used Jones-Wilkins-Lee (JWL) equation. This equation is shown below and each coefficient is shown in Table 3.

JWL equation

$$P_{JWL} = A \left[1 - \frac{\omega}{VR_1} \right] \exp(-R_1 V) + B \left[1 - \frac{\omega}{VR_2} \right] \exp(-R_2 V) + \frac{\omega e}{V}$$

$V = \rho_0$ (Initial density of an explosive) / ρ (Density of detonation gas) P_{JWL} : Pressure
 e : Specific internal energy A, B, R_1, R_2, ω : JWL parameter

Table 3. JWL parameter of PETN (detonation cord)

A(GPa)	B(GPa)	R₁	R₂	ω
180	3.54	5.86	1.40	0.25

About the handling of the detonation phenomenon in this analysis, "C-J Volume Burn" was used. In C-J Volume Burn, the decomposition rate W of the explosive was calculated with the specific volume of the cell, and the detonation state of a cell determines by the decomposition rate of each cell. The decomposition rate of the explosive was calculated by the following formula.

$$W = 1 - \frac{V_0 - V}{V_0 - V_{CJ}}$$

Where V_0 is initial specific volume of the explosive, and V_{CJ} is specific volume of C-J state of the explosive. Then P is the pressure in the cell and P_{JWL} given from JWL equation.

$$P = (1 - W) P_{JWL}$$

EOS Grüneisen

The equation of state for anvil (SUS304) in this study was used Grüneisen equation. This equation is shown below and each coefficient is shown in Table 4.

Grüneisen equation

$$P = \frac{\rho_0 C^2 \mu \left[1 + \left(1 - \frac{\gamma_0}{2} \right) \mu - \frac{a}{2} \mu^2 \right]}{\left[1 - (S_1 - 1) \mu - S_2 \frac{\mu^2}{\mu + 1} - S_3 \frac{\mu^3}{(\mu + 1)^2} \right]^2} + (\gamma_0 + a \mu) e$$

$\eta = \{ 1 - \rho(\text{Density of the medium}) \} / \rho_0$ (Initial density of the medium)

P : Pressure

e : Specific internal energy

a : the first order volume correction to γ_0

C_0, S, S_1, S_2 : Constant of material

γ_0 : Grüneisen coefficient

Table 4. Grüneisen parameter of SUS304

$\rho(\text{kg/m}^3)$	s	$C_0(\text{m/s})$	γ_0
7900	1.49	4570	2.17

6.The Results and Discussion

The pressure distribution diagrams are shown in figure 8. We can observe the collision point to X direction and bonding area for bottom view of $t=6.5, 7.0, 7.5\mu\text{s}$.

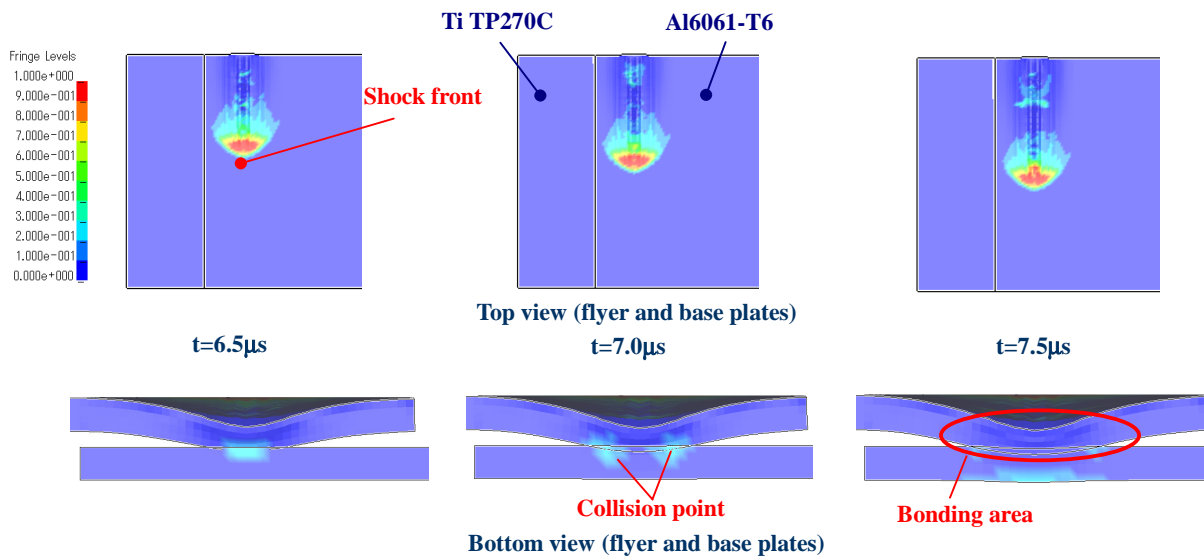
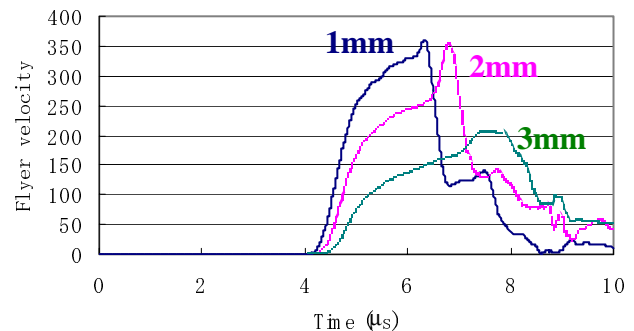
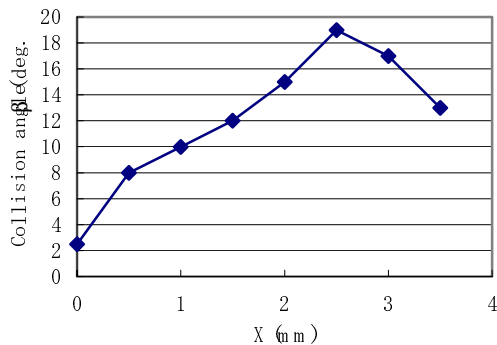


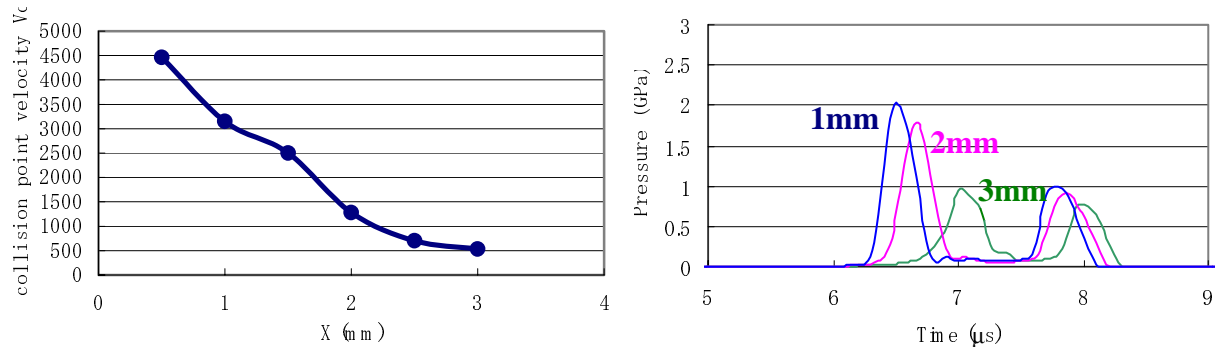
Figure 8. The pressure distribution diagrams

The distribution of collision angle β versus the position X for $Y=5\text{mm}$ is shown in Figure 9 and the flyer velocity V_p to X direction for $Y=5\text{mm}$ is shown in figure 10. Also the figure 11 shows collision point velocity V_c to X direction.



(Left) Figure 9. Distribution of collision angle β versus the each position to X direction for $Y=5\text{mm}$

(Right) Figure 10. The flyer velocity V_p to X direction for $Y=5\text{mm}$

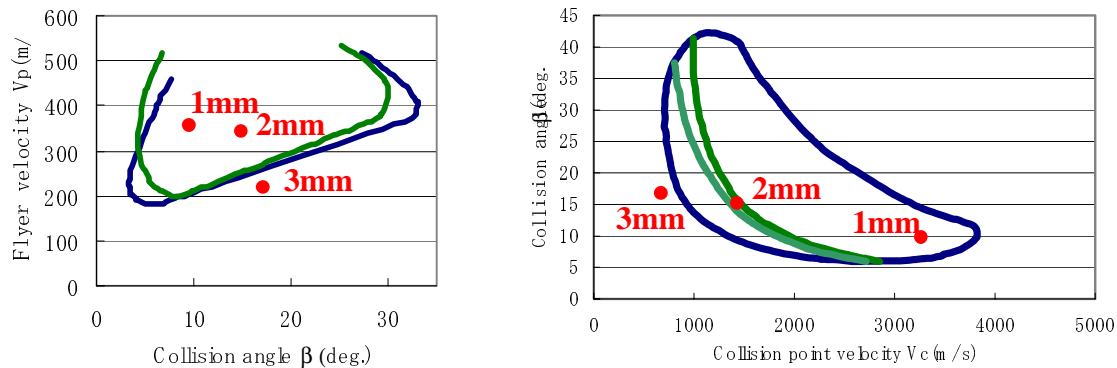


(Left) Figure 11. The collision point velocity versus the each position to X direction for Y=5mm

(Right) Figure 12. The pressure histories on the surface of base plate versus the each position to X direction

Figure 12 shows the pressure histories on surface of base plate versus the each position to X direction for Y=5mm.

The weldability window plotted points obtained by numerical simulation for X=1,2,3mm are shown in figure 13,14.



(Left) Figure 13. Weldability window plotted points for X=1,2,3mm (the relation of β and V_p)

(Right) Figure 14. Weldability window plotted points for X=1,2,3mm (the relation of β and V_c)

From figure 8 we can observe the collision points to X direction at bottom view and the shock front on the flyer plate from top view. The collision points move from center axis (X=0mm) to positive and negative X direction. The time passed the impact between flyer and base plates are stopped and formed one steady width bonding zone.

The collision angle β is increased from 0 to 2.5mm and is decreased more than 2.5mm from figure 9. It is assumed that the flow of explosive gas account for the change of β . We could observe same tendency that the velocity of flyer plate is decreased between 2mm and 3mm in figure 10. From figure 11 the collision point velocity to X direction is decreased with increase of X. The reason is that the higher collision angle the lower collision point velocity and also the

flow of detonation gas influence it, too. From figure 12 we can observe that the value of pressure acting on surface of base plate is about from 1 to 2GPa between X=1mm and 3mm. Still, it is not clear the value of pressure to accomplish the good bonding for TI TP270C and Al6061-T6. We will work to clear the relation between acting pressure and welding aftertime.

In both figures 13, 14 the X=1,2mm points are included weldability range and 3mm is out of range. We can assume that the bonding range is between X=1mm and 3mm from this results. We assumed if more high energy explosive is applied this experiment, we could obtain more good results about some metal combinations.

7. Conclusion

In this study we work on the welding for similar and dissimilar lightweight metal plates using the method of explosive line welding. In consequence we could observe good bonding in both cases of similar and dissimilar metal plates by experiments. Also We presented the numerical simulation for understanding the features of explosive line welding. The calculation include of the problem with propagation of shockwave and collision of the flyer plate into the base plate under shock loading. About flyer and base plate the deformation processes could be observed. We calculated the moving velocity of collision points and flyer plate. From these results we plotted the points in weldability window for the relation of β and V_p or V_c . We could assume the wavy bonding area from this figure. In case of some metal combinations we couldn't weld, the reason is assumed that the shortage of energy influenced it.

References

- Mark L. Wilkins : Computer Simulation of Dynamic Phenomena (1998)
- E. L. Lee, M. Finger and W. Collins : JWL Equation of state Coefficients for High Explosives
Lawrence Livermore Laboratory, UCID-16189 (1973)
- Charles L. Mader : Numerical modeling of explosives and propellants
- Joans A. Zukas, William P. Walters : Explosive Effects and Applications
- D. Meuken and E.P. Carton : Explosive welding and cladding
- E.P. Carton and S. Itoh : Explosive spot, line and seam welding of metal sheets
- Hirofumi Iyama : Deformation and collision process of metal plate on explosive welding using underwater shock wave